

Correlative Evolutions of ENSO and the Seasonal Cycle in the Tropical Pacific Ocean

HENG XIAO AND CARLOS R. MECHOSO

Department of Atmospheric and Oceanic Sciences, University of California, Los Angeles, Los Angeles, California

(Manuscript received 24 July 2007, in final form 13 October 2008)

ABSTRACT

This study examines whether shifts between the correlative evolutions of ENSO and the seasonal cycle in the tropical Pacific Ocean can produce effects that are large enough to alter the evolution of the coupled atmosphere–ocean system. The approach is based on experiments with an ocean general circulation model (OGCM) of the Pacific basin, in which the seasonal and nonseasonal (interannually varying) components of the surface forcing are prescribed with different shifts in time. The shift would make no difference in terms of ENSO variability if the system were linear. The surface fluxes of heat and momentum used to force the ocean are taken from 1) simulations in which the OGCM coupled to an atmospheric GCM produces realistic ENSO variability and 2) NCEP reanalysis data corrected by Comprehensive Ocean–Atmosphere Data Set climatology for the 20-yr period 1980–99. It is found that the response to the shifts in terms of eastern basin heat content can be 20%–40% of the maximum interannual anomaly in the first experiment, whereas it is 10%–20% in the second experiment. In addition, the response to the shift is event dependent. A response of this magnitude can potentially generate coupled atmosphere–ocean interactions that alter subsequent event evolution. Analysis of a selected event shows that the major contribution to the response is provided by the anomalous zonal advection of seasonal mean temperature in the equatorial band. Additional OGCM experiments suggest that both directly forced and delayed signals provide comparable contributions to the response. An interpretation of the results based on the “delayed oscillator” paradigm and on equatorial wave–mean flow interaction is given. It is argued that the same oceanic ENSO anomalies in different times of the oceanic seasonal cycle can result in different ENSO evolutions because of nonlinear interactions between equatorially trapped waves at work during ENSO and the seasonally varying upper-ocean currents and thermocline structure.

1. Introduction

A better understanding of ENSO evolution requires a deeper insight into its interactions with the seasonal cycle of the climate system in the tropical Pacific Ocean. ENSO studies performed with numerical models of intermediate complexity have suggested several mechanisms for such interactions (e.g., Battisti 1988; Tziperman et al. 1997; Clement et al. 1999, 2000; Fedorov and Philander 2001; Timmermann et al. 2005) and even argued that they are essential components of the observed interannual variability (Jin et al. 1996). The mechanisms of interaction include the nonlinearities that can arise if surface wind components and/or

sea surface temperatures are obtained by superposition of the seasonal cycle and interannual anomalies (Tziperman et al. 1997).

Typical intermediate coupled models used in ENSO research only include seasonal variations in the oceanic surface layer and lower atmosphere mean condition. Intermediate models with modifications that allow for effects by seasonal variations in other features of the upper-ocean circulation (e.g., the thermocline) and GCMs capable of producing a realistic seasonal cycle in the upper ocean have been used to explore the interactions between ENSO and the seasonal cycle in the upper ocean (e.g., Chang et al. 1995; Guilyardi 2006). An and Wang (2001), for example, working with a modified Cane–Zebiak model, found that allowing the basic state thermocline depth (upper-layer depth) to vary seasonally renders the timing of La Niña events more realistic than in the standard model version. Guilyardi et al. (2003) proposed that, in ENSO events

Corresponding author address: Heng Xiao, Department of Atmospheric and Oceanic Sciences, University of California, Los Angeles, 7127 Math Sciences Bldg., 405 Hilgard Ave., Los Angeles, CA 90095-1565.
E-mail: hengx@atmos.ucla.edu

simulated by a coupled GCM (CGCM), advection into the equatorial region of heat content anomalies by the seasonally varying western boundary current (WBC) contributes to event demise and thus to phase locking because the WBC is strongest toward the end of the year. Vintzileos et al. (1999a,b), also using a CGCM, hypothesized that the seasonal cycle of the equatorial undercurrent and meridional circulation cells plays an important role in the redistribution of ENSO heat content anomalies.

The primary goal of this study is to examine whether shifts between the correlative evolutions of ENSO and the seasonal cycle in the tropical Pacific Ocean can produce effects that are large enough to alter the evolution of the coupled atmosphere–ocean system. We aim, therefore, to assess the importance of processes absent in typical intermediate coupled models of ENSO and to test hypotheses proposed by works using modified intermediate models and CGCMs. We follow an approach based on uncoupled ocean GCM (OGCM) simulations. In this framework, we can modify the phase relationship between interannual anomalies and the seasonal cycle of the surface forcing in a relatively simple but also realistic way. The approach selected does not include coupled feedbacks. In view of this demerit, we can only search for responses that generate coupled atmosphere–ocean interactions with the potential to alter the future event evolution.

We start in section 2 with a description of the model and experimental design. Section 3 presents the results of the experiments with shifts between the phases of interannual anomalies and the seasonal cycle. Section 4 discusses the impact of direct and remote mechanisms on the response to the shifts. The conclusions are in section 5.

2. Model and experiment design

The OGCM we use is the Pacific basin (30°S–50°N) version of the Modular Ocean Model (MOM, version 1.1), configured with 27 layers in the vertical direction and a horizontal resolution of $1/3^\circ$ latitude by 1° longitude equatorward of 10° , increasing to 3° by 1° at higher latitudes. We have previously coupled this OGCM to the University of California, Los Angeles, atmospheric GCM [version 6.8, 15 levels in the vertical direction and a horizontal resolution of 4° latitude by 5° longitude; see Yu and Mechoso (2001) for more details].

As a first step, we spin up the OGCM by running it for 10 yr using mean seasonal surface fluxes and wind stresses from the CGCM simulation reported in Yu and Mechoso (2001). The OGCM is restarted and run using the full surface fluxes from the same CGCM sim-

ulation for the 16-yr-long period during which the output is currently available. The forcing fields are obtained by linear interpolation to the OGCM time step of monthly-mean CGCM output assigned at half month. To compensate for unrealistic behaviors in long runs caused by this approximation, we add a relatively weak (30 day) relaxation of surface temperature and salinity to the CGCM climatology. We refer to this 16-yr OGCM simulation as the CONTROL-CGCM run. On the one hand, our procedure assures consistency between forcing and internal fields in the ocean model. On the other hand, our results will be affected by “imperfections” in the CGCM simulation. For example, the meridional structure of the simulated ENSO is, in general, narrower in latitude than in the observation. In addition, the simulated variability in the far western basin is too strong. Our previous studies, however, have shown that the simulated interannual variability is comparable to observation both in terms of temporal behavior and spatial patterns in the central and eastern equatorial Pacific basin (Yu and Mechoso 2001; Mechoso et al. 2003). Hence, we believe that such imperfections do not pose an important challenge to our approach.

Next we perform an OGCM experiment by changing the phase difference between interannual anomalies and seasonal cycle of the surface fluxes by 0.5 yr—that is, by applying the anomalous fluxes with a 6-month delay (i.e., shifting). In this experiment, which we call SHIFT-CGCM, the surface fluxes for October of a particular year, for example, are obtained by adding the anomalous fields corresponding to this month to the mean seasonal fluxes of April. Our method, therefore, is similar to that of Xie (1995), except that to force the OGCM we use model-generated or reanalysis fields whereas he uses idealizations that are symmetric about the equator and zonally uniform. Xie (1995) found a significant response to the shift in SST and suggested that amplification of the response by interactions with the atmosphere can contribute to ENSO’s phase locking to the seasonal cycle.

Because a 16-year period is relatively short in reference to the ENSO time scale, we performed another 43-yr-long simulation with the CGCM and repeated the entire procedure, thus obtaining two additional 43-yr-long OGCM simulations that we call the CONTROL-CGCM* and SHIFT-CGCM*.

The control and shift experiments are repeated using National Centers for Environmental Prediction (NCEP) reanalysis data (corrected by the Comprehensive Ocean–Atmosphere Data Set long-term mean) for the period of 1980–99. These experiments are labeled CONTROL-NCEP and SHIFT-NCEP, respectively.

3. Results of the SHIFT experiments

Figure 1 shows the monthly-mean temperature anomalies averaged in the upper ocean (0–300 m) along the equator obtained in CONTROL-CGCM. There are two major ENSO events in the period, of which one is warm (marked ELN) and the other is cold (LAN). The heat content anomalies in the western and eastern parts of the basin during the events appear out of phase, as is typical in observed ENSO events. Figure 2 shows the monthly-mean temperature anomalies in the upper ocean at the center of the Niño-3 region (equator, 110°W) in the CONTROL-CGCM and SHIFT-CGCM experiments for ELN and LAN, together with the corresponding responses to the 6-month shift. In ELN, the magnitude of the response in heat content anomaly to the shift reaches 40% of the maximal anomaly for the event, and more than half of the total anomaly for that month (October of the fourth year). In LAN, the response of the heat content anomaly is about half of that in ELN. In a coupled scenario, responses of this magnitude can generate atmosphere–ocean interactions that would alter the future event evolution.

In CONTROL-CGCM* there are eight warm and nine cold ENSO events in total, of which two are very weak. We also find responses to the shift larger than 30% in at least half of the events. In Fig. 3 we show the responses to the shift in terms of heat content anomaly at 110°W on the equator from four representative cases, including two warm (Figs. 3b,c) and two cold cases (Figs. 3a,d). Here the response reaches magnitudes up to 50% of the monthly anomalies. In Figs. 3b and 3c, the responses are similar to those we found in the ELN case. In Figs. 3a and 3d, we find larger responses to the shift during La Niña events when compared with those in the LAN case discussed above. The response to the shift in some simulated ENSO events, therefore, is a robust feature of our results. The considerable event-to-event variation is another robust feature. In the remainder of this paper we concentrate on CONTROL-CGCM and SHIFT-CGCM.

Before performing further analysis, we test the robustness of the response obtained in the ELN case. We use two methods. In the first, we make several shorter SHIFT runs (4 yr long) for the ELN case with different initial conditions. These are produced by simply varying the period of anomalous forcing applied before the initiation of the event. For the ELN case, in which SST anomalies peak during the second half of year 4, we perform 6-month shift experiments by starting from spinup conditions and applying anomalous forcings from different times in years 1 and 2 of CONTROL-CGCM. A comparison between Fig. 4a and Fig. 3 shows

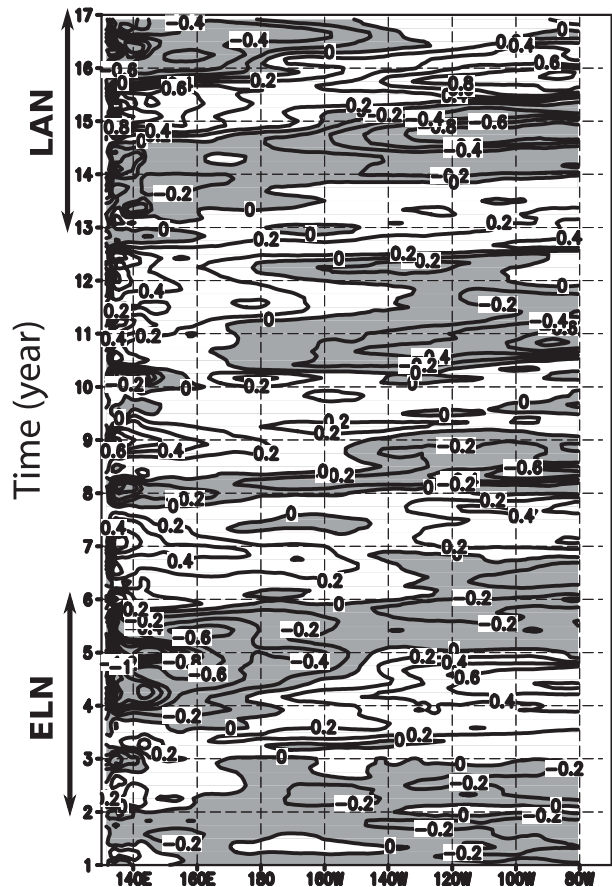


FIG. 1. Vertical mean (0–300 m) temperature anomaly along the equator in CONTROL-CGCM. The contour interval is 0.2°C, and negative anomalies are shaded. Cases ELN and LAN are the two major events in this run.

that the response to the shift is much larger than the responses to small perturbations in the oceanic initial condition. In the second test, we change the magnitude of the shift from 6 months to 3 months and then to 9 months. The responses to the 3-month and 9-month shifts are almost as strong as that to the 6-month shift (Fig. 4b), although there are differences in detail.

The response to the shift is event dependent. We further illustrate such dependence by using two simple indicators of the basinwide heat content redistribution in the upper equatorial Pacific (5°S–5°N, 0–300 m). These indices are defined as the average and difference temperature anomaly between the equatorial regions west and east of 150°W and represent the zonal mean heat content anomaly of the equatorial band and the anomalous zonal tilt of the equatorial thermocline, respectively. Figure 5 shows the time evolution of both indices in ELN and LAN for both CONTROL-CGCM and SHIFT-CGCM. ELN shows a clear response to the shift in the thermocline tilt index, whereas LAN shows a

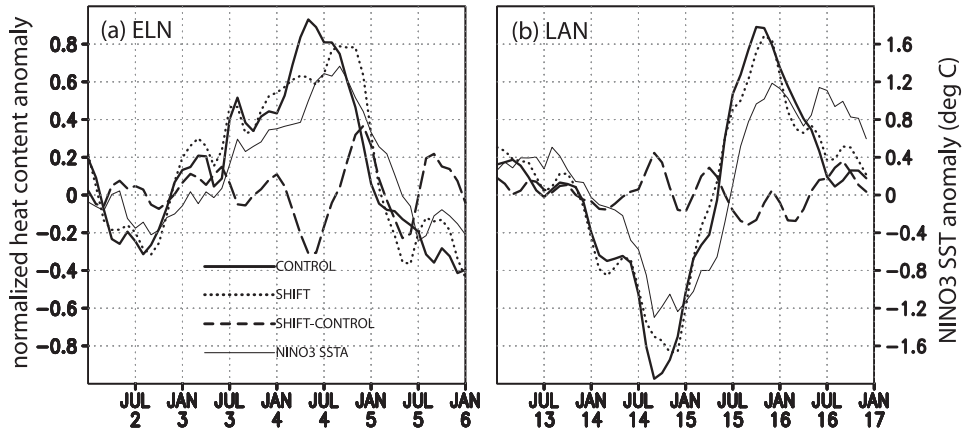


FIG. 2. Vertical mean (0–300 m) temperature anomaly ($^{\circ}\text{C}$) for (a) case ELN and (b) case LAN at the equator and 110°W for CONTROL-CGCM (thick solid lines) and SHIFT-CGCM (dotted lines), and their difference (dashed lines). All values are normalized by the maximal monthly anomaly in the CGCM simulation. The thin solid lines represent the Niño-3 SST anomalies ($^{\circ}\text{C}$) in the CGCM simulation for the corresponding periods.

much smaller response in both indices. The response in zonal-averaged anomaly is negligible for both events. (Similar results are found for CONTROL-CGCM* and SHIFT-CGCM*.) We will discuss the weak response in the zonal-averaged anomaly later in the paper.

To further examine the origin of the large response in ELN, we study the heat transport into the eastern equatorial box (5°S – 5°N , 150°W to the coast, 0–300 m). A calculation of the heat budget of the region shows

that horizontal heat transport is the dominant term, as in Philander and Hurlin (1988) and others. As shown in Fig. 6, almost all of the difference in heat transport into the eastern part of the basin between CONTROL-CGCM and SHIFT-CGCM is due to the different contribution by advection of mean temperature by the anomalous zonal current.

Figure 7 shows the difference between CONTROL-NCEP and SHIFT-NCEP in terms of heat content at

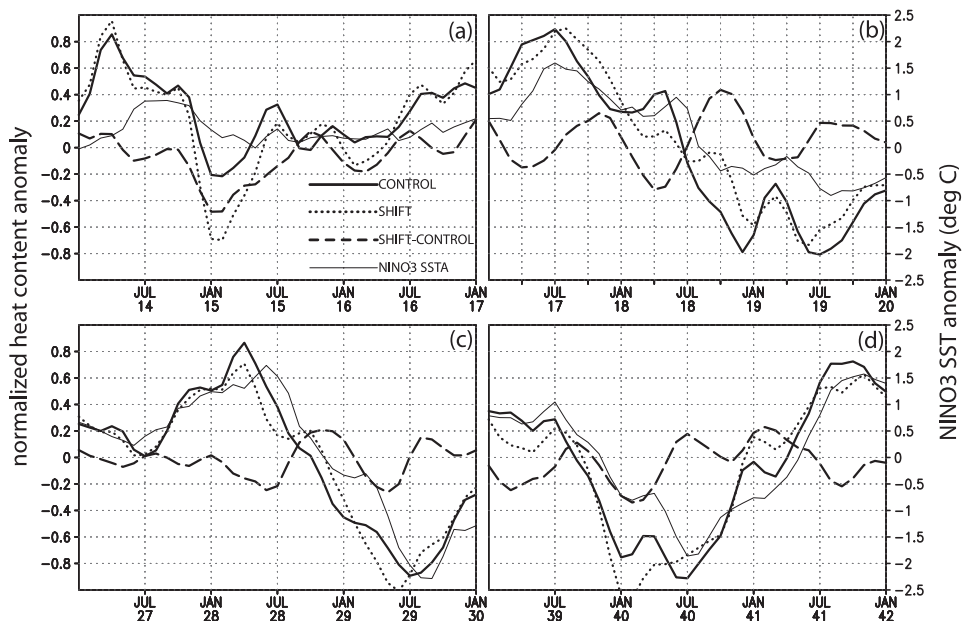


FIG. 3. As in Fig. 2, but for CONTROL-CGCM* and SHIFT-CGCM*: (a) January (Jan) of year (yr) 14–Jan of yr 17, (b) Jan of yr 17–Jan of yr 20, (c) Jan of yr 27–Jan of yr 30, and (d) Jan of yr 39–Jan of yr 42. All values are normalized by the maximal monthly anomaly in each panel.

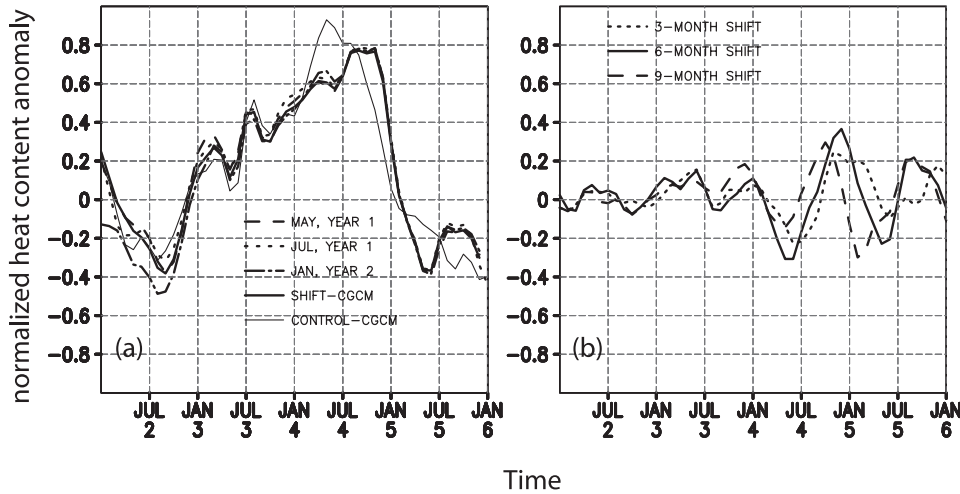


FIG. 4. (a) Vertical mean (0–300 m) temperature anomaly ($^{\circ}\text{C}$) at the equator and 110°W in shift runs for case ELN from three different initial conditions, together with those from SHIFT-CGCM and CONTROL-CGCM. (b) Responses to 3-, 6-, and 9-month shifts in the ELN case from the same initial condition. All values are normalized by the maximal monthly anomaly in the CGCM simulation.

110°W on the equator in the same format as Figs. 2 and 3. The values in Fig. 7 correspond to the heat content anomaly normalized by the maximal anomaly in the period of each panel. We note that the response to the shift is nonlinear in ENSO amplitude. For example, the response in the very strong 1997/98 warm event is relatively small ($\sim 10\%$) in comparison with that in the weaker 1988/89 cold event ($>20\%$). Furthermore, the response in this set of experiments seems to be systematically smaller than that in the set forced with CGCM output, which can reach 50% in some cases.

4. Direct and delayed effects

In this section we estimate the contribution of “direct or local” and “delayed or remote” effects to the differences between CONTROL-CGCM and SHIFT-CGCM. We focus on October of the fourth year, when differences in the ELN case have largest magnitudes. First, we perform several October simulations using the anomalous forcing corresponding to the fourth year of CONTROL-CGCM applied at increasingly earlier times, before which the forcings do not have interannual variability. We do this by taking initial conditions from

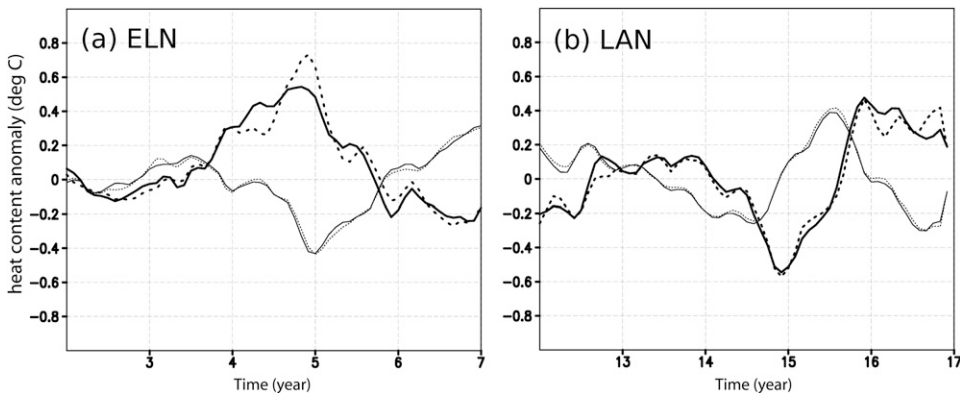


FIG. 5. Average temperature anomaly ($^{\circ}\text{C}$) between the eastern and western parts of the equatorial basin (5°S – 5°N , 0–300 m) for CONTROL-CGCM (thick solid line) and SHIFT-CGCM (thick dotted line), along with the difference between the two parts for CONTROL-CGCM (thin solid line) and SHIFT-CGCM (thin dotted line), for (a) case ELN and (b) case LAN.

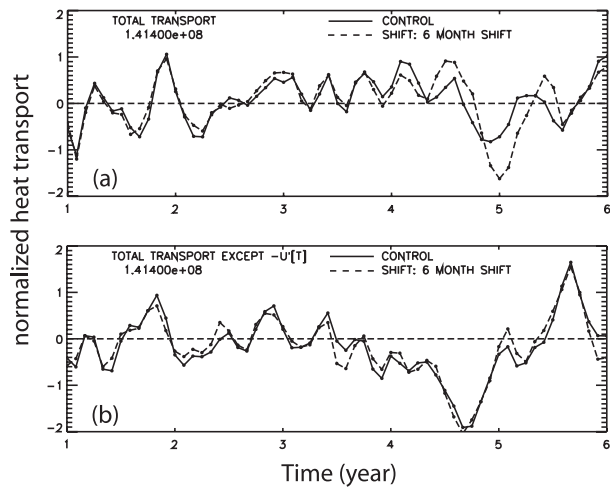


FIG. 6. (a) Horizontal heat transport into the eastern half of the equatorial band (5°S–5°N, 150°–70°W, 0–300 m) for case ELN in CONTROL-CGCM (solid line) and SHIFT-CGCM (dashed line). (b) As in (a), except that transport by anomalous zonal advection of seasonal mean temperature is not included. All values are normalized by $1.414 \times 10^8 \text{ (m}^3 \text{ °C}^{-1} \text{ s}^{-1}\text{)}$.

the spinup run (i.e., obtained without interannual variations in the surface fluxes) corresponding to n months before the last 1 October in the spinup run. The simulations performed are referred to as CONTROL- n experiments. Next, we repeat the simulations with the seasonal cycle shifted, as we did in the previous section of the paper. This is done by starting the simulations with initial conditions (from the spinup run) corresponding to n months before the last 1 April in the spinup run and using exactly the same anomalous surface fluxes as in the corresponding CONTROL- n experiment. We refer to these runs as SHIFT- n . The larger the n is, the more we see the impact of delayed or remote effects. In this manner, we make five pairs of OGCM experiments corresponding to $n = 1, 3, 6, 9,$ and 12 (i.e., going back by 3-month intervals).

Figure 8 presents a summary of results in terms of differences in anomalous zonal velocities at the equator, together with the difference between CONTROL-CGCM and SHIFT-CGCM in October of the fourth year. We focus on the central basin from the surface to

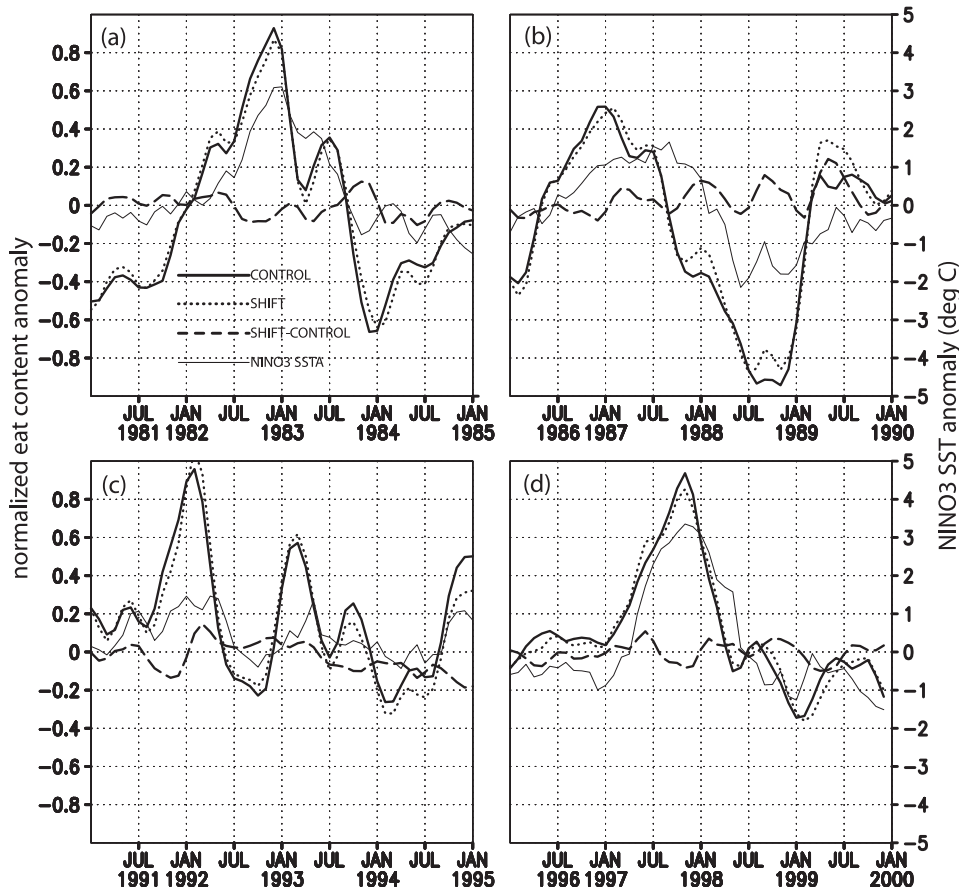


FIG. 7. As in Fig. 3, but for CONTROL-NCEP and SHIFT-NCEP: (a) 1981–85, (b) 1986–90, (c) 1991–95, and (d) 1996–2000.

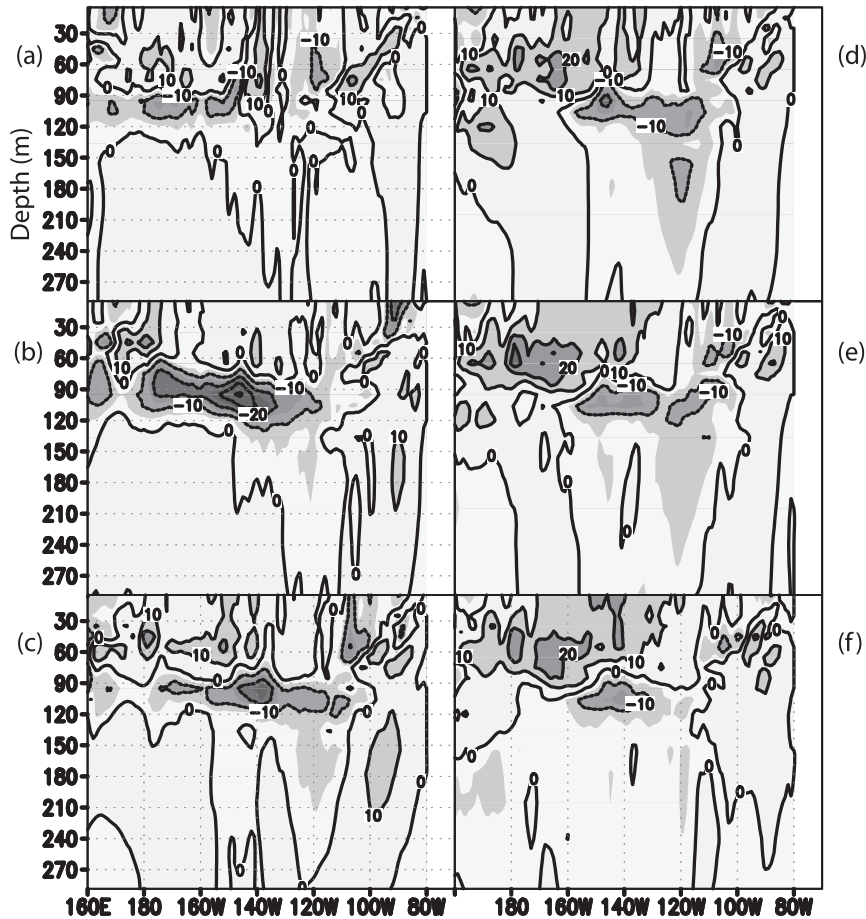


FIG. 8. The difference in zonal current anomaly (cm s^{-1}) at the equator for October of the fourth year between (a) CONTROL-1 and SHIFT-1, (b) CONTROL-3 and SHIFT-3, (c) CONTROL-6 and SHIFT-6, (d) CONTROL-9 and SHIFT-9, (e) CONTROL-12 and SHIFT-12, and (f) CONTROL-CGCM and SHIFT-CGCM. The contour interval is 10 cm s^{-1} .

about 100 m deep. The panel for $n = 1$ (Fig. 8a) shows that local effects explain a significant part of the difference between CONTROL-CGCM and SHIFT-CGCM (Fig. 8f). An inspection of the entire panel sequence (Figs. 8a–e) clearly shows that the differences between CONTROL-CGCM and SHIFT-CGCM (Fig. 8f) in the upper ocean are practically recovered for $n \geq 9$ and not for smaller n . This indicates a comparable contribution of both local (direct) and remote (delayed) effects to the response to the shift in terms of anomalous zonal currents, which are primarily responsible for the difference in heat transport as shown in Fig. 6.

5. Discussion and conclusions

Our study starts with a direct estimation of the impact on an OGCM simulation of shifting by 6 months the phase relationship between the seasonally and inter-

annually varying components of the prescribed monthly mean surface fluxes. These were produced by the same model when it was coupled to an AGCM. In this way, the anomalies in surface fluxes corresponding to the northern autumn are applied simultaneously with the seasonal fields for the northern spring. The method used is similar to that used by Xie (1995), who found significant effects of the shift on SST in idealized OGCM experiments.

According to the results, the shift produces differences in eastern basin heat content that reach up to 20%–40% of the interannual anomaly in at least half of the events. The response is case dependent. A heat transport analysis of one case in which the response is large shows that the process most affected is the anomalous zonal advection of seasonal thermocline in the midbasin.

If the OGCM is forced with surface fluxes corresponding to the NCEP reanalysis for the period 1980–99, then the response to the shift is on the order of

10%–20% of the maximal ENSO anomaly. There are also interevent variations in the response. Another common feature of the experiments with surface fluxes from the CGCM simulation and NCEP reanalysis data is that the zonal mean heat content at the equator is insensitive to the shift (cf. Fig. 2). This indicates that seasonal features such as variation in the advection of heat content anomalies by the WBC into the equatorial band, which changes the zonal mean heat content, are either unimportant or are balanced by other processes that counteract such effects. The responses we found in the experiments with surface fluxes from the NCEP reanalysis tend to be smaller than those in the experiments that are forced by CGCM output. The relatively short length of experiments and observational datasets in reference to the ENSO time scale may not be long enough to argue for a systematic difference between simulation and observations in view of the large event-to-event variability.

The selected warm-event case in the runs with surface fluxes from the CGCM output is analyzed further to examine the relative contributions to the response of direct and delayed effects. This is done by tracing the impact of anomalous forcing back in time with and without the shift. The results show that 1) direct or local response to the anomalous forcings contributes significantly to the difference between the control and shift experiments and 2) delayed responses associated with anomalous forcings applied 9–12 months earlier are partly responsible for the difference between the control and the shift experiments.

Our study finds, therefore, that an artificial shift in the phase relationship between the seasonal and interannual components of the surface fluxes (monthly mean) in an OGCM can cause responses up to 50% in terms of heat content anomaly in the equatorial eastern basin. The response is due to changes in the anomalous zonal advection of seasonal mean temperature in the equatorial upper ocean. Furthermore, these changes are due to both local and remote effects set by the shift and can only be interpreted in a nonlinear framework. The same oceanic ENSO anomalies in different times of the seasonal cycle can, therefore, result in different ENSO evolutions.

To interpret our results, let us start by considering the “delayed oscillator” paradigm of ENSO. According to this paradigm, there are two kinds of signals causing thermocline change in the equatorial eastern basin during ENSO: 1) Kelvin waves directly forced in the central to western equatorial basin 1–2 months earlier (direct signals) and 2) Kelvin waves generated by reflection of slowly propagating Rossby waves generated much earlier (remote signals). Our analysis finds

that both local and remote effects of the anomalous forcings are responsible for the difference between the control and the shift experiments. Thus, both kinds of wave signals in the delayed-oscillator paradigm are influenced by the shift, because they are being forced and propagating under different seasonal mean conditions. These arguments are consistent with several previous studies on how features of the equatorial Pacific mean state can affect equatorially trapped, low-frequency baroclinic Kelvin and Rossby waves (e.g., McPhaden and Ripa 1990; Giese and Harrison 1990; Long and Chang 1990; Zheng et al. 1998). The seasonal variation in major equatorial currents in the upper ocean and the equatorial thermocline slope continuously affects equatorial waves excited by ENSO wind anomalies. The accumulated effect of the seasonal variation on these waves can be very significant, as in the ELN case examined here. However, given the unique temporal and spatial patterns of each individual event, this accumulated effect may be weak, as in the LAN case examined here.

The seasonal variation in the lower atmosphere and oceanic mixed layer results in seasonal variations of the coupling instability and regulates the delayed oscillator (Tziperman et al. 1998). Our results imply that the seasonal variation in the upper-ocean currents and thermocline slope have a similar regulating effect. Yang and O’Brien (1993) showed with an intermediate coupled model of ENSO that increasing the steepness of the thermocline slope from the central basin to the eastern basin could decrease the model’s interannual variability (and vice versa) because of impacts on Kelvin wave propagation. Our results, obtained in a more complex and realistic framework, are consistent with such impacts on ENSO evolution.

Acknowledgments. This research was supported by NOAA under Grant NA66GP0370. We gratefully acknowledge the helpful comments from two anonymous reviewers.

REFERENCES

- An, S.-I., and B. Wang, 2001: Mechanisms of locking of the El Niño and La Niña mature phases to boreal winter. *J. Climate*, **14**, 2164–2176.
- Battisti, D. S., 1988: Dynamics and thermodynamics of a warming event in a coupled tropical atmosphere–ocean model. *J. Atmos. Sci.*, **45**, 2889–2919.
- Chang, P., L. Ji, B. Wang, and T. Li, 1995: Interactions between the seasonal cycle and El Niño–Southern Oscillation in an intermediate coupled ocean–atmosphere model. *J. Atmos. Sci.*, **52**, 2353–2372.
- Clement, A. C., R. Seager, and M. A. Cane, 1999: Orbital controls on the El Niño/Southern Oscillation and the tropical climate. *Paleoceanography*, **14**, 441–456.

- , —, and —, 2000: Suppression of El Niño during the mid-Holocene by changes in the earth's orbit. *Paleoceanography*, **15**, 731–737.
- Fedorov, A. V., and S. G. H. Philander, 2001: A stability analysis of tropical ocean–atmosphere interactions: Bridging measurements and theory for El Niño. *J. Climate*, **14**, 3086–3101.
- Giese, B. S., and D. E. Harrison, 1990: Aspects of the Kelvin wave response to episodic wind forcing. *J. Geophys. Res.*, **95**, 7289–7312.
- Guilyardi, E., 2006: El Niño–mean state–seasonal cycle interactions in a multi-model ensemble. *Climate Dyn.*, **26**, 329–348.
- , P. Delecluse, S. Gualdi, and A. Navarra, 2003: Mechanisms for ENSO phase change in a coupled GCM. *J. Climate*, **16**, 1141–1158.
- Jin, F.-F., J. D. Neelin, and M. Ghil, 1996: El Niño/Southern Oscillation and the annual cycle: Subharmonic frequency-locking and aperiodicity. *Physica D*, **98**, 442–465.
- Long, B., and P. Chang, 1990: Propagation of an equatorial Kelvin wave in a varying thermocline. *J. Phys. Oceanogr.*, **20**, 1826–1841.
- McPhaden, M. J., and P. Ripa, 1990: Wave–mean flow interactions in the equatorial ocean. *Annu. Rev. Fluid Mech.*, **22**, 167–205.
- Mechoso, C. R., J. D. Neelin, and J.-Y. Yu, 2003: Testing simple models of ENSO. *J. Atmos. Sci.*, **60**, 305–318.
- Philander, S. G. H., and W. J. Hurlin, 1988: The heat budget of the tropical Pacific Ocean in a simulation of the 1982/83 El Niño. *J. Phys. Oceanogr.*, **18**, 926–931.
- Timmermann, A., S.-I. An, U. Krebs, and H. Goosse, 2005: ENSO suppression due to weakening of the North Atlantic thermohaline circulation. *J. Climate*, **18**, 3122–3139.
- Tziperman, E., S. E. Zebiak, and M. A. Cane, 1997: Mechanisms of seasonal–ENSO interaction. *J. Atmos. Sci.*, **54**, 61–71.
- , M. A. Cane, S. E. Zebiak, Y. Xue, and B. Blumenthal, 1998: Locking of El Niño's peak time to the end of the calendar year in the delayed oscillator picture of ENSO. *J. Climate*, **11**, 2191–2199.
- Vintzileos, A., P. Delecluse, and R. Sadourny, 1999a: On the mechanisms in a tropical ocean–global atmosphere coupled general circulation model. Part I: Mean state and the seasonal cycle. *Climate Dyn.*, **15**, 43–62.
- , —, and —, 1999b: On the mechanisms in a tropical ocean–global atmosphere coupled general circulation model. Part II: Interannual variability and its relation to the seasonal cycle. *Climate Dyn.*, **15**, 63–80.
- Xie, S.-P., 1995: Interaction between the annual and interannual variations in the equatorial Pacific. *J. Phys. Oceanogr.*, **25**, 1930–1940.
- Yang, J., and J. J. O'Brien, 1993: A coupled atmosphere–ocean model in the tropics with different thermocline profiles. *J. Climate*, **6**, 1027–1041.
- Yu, J.-Y., and C. R. Mechoso, 2000: A coupled atmosphere–ocean GCM study of the ENSO cycle. *J. Climate*, **14**, 2329–2350.
- Zheng, Q., R. D. Susanto, X.-H. Yan, W. T. Liu, and C.-R. Ho, 1998: Observation of equatorial Kelvin solitary waves in a slowly varying thermocline. *Nonlinear Processes Geophys.*, **5**, 153–165.